The Influence of Halides in Polyoxotitanate Cages; Dipole Moment, Splitting and Expansion of d-orbitals and Electron-Electron Repulsion

Schirin Hanf,[a] Peter D Matthews,*[a,b] Ning Li,[a,c] He-Kuan Luo[c] and Dominic S Wright*[a]

[a] *Department of Chemistry, University of Cambridge, Lensfield Road, Cambridge, CB2 1EW (UK). E-mail: dsw1000@cam.ac.uk*
[b] *School of Chemistry, University of Manchester, Oxford Road, Manchester, M13 9PL (UK). E-mail: peter.matthews-2@manchester.ac.uk*
[c] *Institute of Materials Research and Engineering, Agency for Science, Technology and Research, 2 Fusionopolis Way, #08-03, Innovis, Singapore 138634 (Singapore).*

1) **$[Ti_3O(O^iPr)_9X]$ (X = F, Cl, Br, I)**

2) **$[Ti_4O(OEt)_{15}CoX]$ (X = F, Cl, Br, I) and $[Ti_4O(OEt)_{14}(HOEt)]$**

3) **$[Ti_7O_5(OEt)_{19}CoX]$ (X = F, Cl, Br, I) and $[Ti_7O_4(OEt)_{20}]$**

4) **Diffuse reflectance UV-vis spectroscopy**

5) **Single-crystal X-ray crystallography**

1) $[Ti_3O(O^iPr)_9X]$

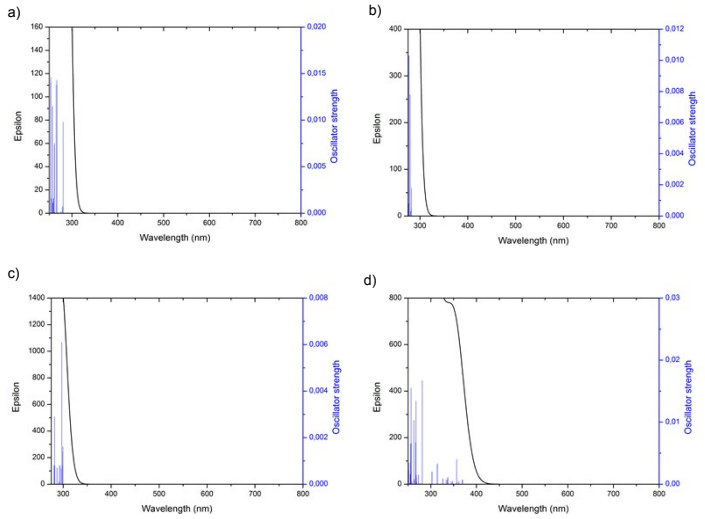

Figure S1: Calculated UV-Vis spectra of $[Ti_3O(O^iPr)_9X]$ X = F (a), Cl (b), Br (c), I (d) using TD-DFT methods (B3LYP/6-31g**, 6-311g** for iodine).

Table S1: Atomic decomposition of molecular orbitals of $[Ti_3O(O^iPr)_9F]$ (B3LYP/6-31g** level of theory).

Orbital	Orbital energy (eV)	Atomic composition (%)			
		Titanium	Oxygen	Fluorine	^{i}Propyl
HOMO	-6.85	1	71	2	1
HOMO-1	-6.85	1	71	2	1
HOMO-2	-7.10	4	66	2	4
LUMO	-1.36	80	14	1	6
LUMO+1	-1.36	80	14	1	5
LUMO+2	-1.22	86	11	0	3
LUMO+3	-1.11	89	19	0	2

Table S2: Atomic decomposition of molecular orbitals of $[Ti_3O(O^iPr)_9Cl]$ (B3LYP/6-31g** level of theory).

Orbital	Orbital energy (eV)	Atomic composition (%)			
		Titanium	Oxygen	Chlorine	^{i}Propyl
HOMO	-6.78	1	47	35	16
HOMO-1	-6.78	1	46	35	16
HOMO-2	-6.97	2	40	44	13
LUMO	-1.37	85	13	0	2
LUMO+1	-1.35	80	14	0	6
LUMO+2	-1.35	80	14	0	6
LUMO+3	-1.27	87	10	0	3

Table S3: Atomic decomposition of molecular orbitals of $[Ti_3O(O^iPr)_9Br]$ (B3LYP/6-31g** level of theory).

Orbital	Orbital energy (eV)	Atomic composition (%)			
		Titanium	Oxygen	Bromine	^{i}Propyl
HOMO	-6.50	3	25	63	8
HOMO-1	-6.50	3	25	63	8
HOMO-2	-6.70	3	33	55	9
LUMO	-1.39	85	13	0	2

LUMO+1	-1.36	80	13	0	6
LUMO+2	-1.36	80	14	0	6
LUMO+3	-1.28	87	10	0	3
LUMO+4	-1.19	83	13	0	4
LUMO+5	-1.19	83	13	0	4

Table S4: Atomic decomposition of molecular orbitals of $[Ti_3O(O^iPr)_9I]$ (B3LYP/6-31g**, 6-311g** for iodine level of theory).

Orbital	Orbital energy (eV)	Atomic composition (%)			
		Titanium	Oxygen	Iodine	^{i}Propyl
HOMO	-5.69	1	5	91	3
HOMO-1	-5.69	1	5	91	3
HOMO-2	-5.97	3	16	79	3
LUMO	-1.51	85	13	0	2
LUMO+1	-1.42	81	13	0	6
LUMO+2	-1.42	81	13	0	6
LUMO+5	-1.29	83	13	0	4
LUMO+6	-1.16	83	14	0	3
LUMO+8	-0.77	78	13	3	6

Table S5: Main orbital contributions to transition of $[Ti_3O(O^iPr)_9F]$ (with oscillator strengths ≥ 0.001). Calculated employing TD-DFT methods (B3LYP/6-31g**).

Main orbital contributions	Eg (eV)	Eg (nm)	Oscillator strength
HOMO-1 → LUMO+1 HOMO → LUMO+2 HOMO-2→ LUMO	4.420	280.5	0.0098
HOMO → LUMO+2	4.634	266.4	0.0143
HOMO → LUMO	4.659	266.1	0.0138
HOMO → LUMO+3	4.752	260.9	0.0075
HOMO-1 → LUMO+3	4.755	260.8	0.0073

Table S6: Main orbital contributions to transition of $[Ti_3O(O^iPr)_9Cl]$ (with oscillator strengths ≥ 0.001). Calculated employing TD-DFT methods (B3LYP/6-31g**).

Main orbital contributions	Eg (eV)	Eg (nm)	Oscillator strength
HOMO-1 → LUMO+1 HOMO → LUMO+2 HOMO-2 → LUMO	4.392	282.3	0.0018
HOMO-1 → LUMO	4.439	279.3	0.0078
HOMO → LUMO	4.439	279.3	0.0077
HOMO → LUMO HOMO → LUMO+3	4.476	277.0	0.0103
HOMO-1 → LUMO HOMO-1 → LUMO+3	4.476	277.0	0.0103

Table S7: Main orbital contributions to transition of $[Ti_3O(O^iPr)_9Br]$ (with oscillator strengths ≥ 0.001). Calculated employing TD-DFT methods (B3LYP/6-31g**).

Main orbital contributions	Eg (eV)	Eg (nm)	Oscillator strength
HOMO → LUMO HOMO → LUMO+1	4.141	299.4	0.0016
HOMO-1 → LUMO	4.144	299.1	0.0014
HOMO-1 → LUMO	4.172	297.2	0.0061
HOMO-1 → LUMO	4.173	297.1	0.0058
HOMO-1 → LUMO+1 HOMO → LUMO+5	4.395	282.1	0.0029

Table S8: Main orbital contributions to transition of $[Ti_3O(O^iPr)_9I]$ (with oscillator strengths ≥ 0.001). Calculated employing TD-DFT methods (B3LYP/6-31g**, 6-311g** for iodine).

Main orbital contributions	Eg (eV)	Eg (nm)	Oscillator strength
HOMO-2 → LUMO+1 HOMO-2 → LUMO+2	3.675	337.4	0.0011
HOMO-2 → LUMO+1 HOMO → LUMO+5	3.677	337.2	0.0011
HOMO-2 → LUMO+6	3.945	314.3	0.0033
HOMO-2 → LUMO+8	4.410	281.2	0.0167

Table S9: Band gaps obtained DOS calculations (B3LYP/6-31g**, 6-311g** for iodine).

Compound	Eg (eV)
1-F	5.49
1-Cl	5.41
1-Br	5.11
1-I	4.18

Table S10: Band gaps obtained from TD-DFT calculations (B3LYP/6-31g**, 6-311g** for iodine). First singlet excitation energy with oscillator strength ≥ 0.

Compound	Main orbital contributions	Eg (eV)	Eg (nm)	Oscillator strength
1-F	HOMO-1 → LUMO+1 HOMO → LUMO	4.420	280.5	0.0098
1-Cl	HOMO-1 → LUMO+1 HOMO → LUMO+2	4.392	282.3	0.0018
1-Br	HOMO → LUMO HOMO → LUMO+1	4.142	299.4	0.0016
1-I	HOMO → LUMO	3.357	369.3	0.0007

2) $[Ti_4O(OEt)_{15}CoX]$ (X = F, Cl, Br, I) and $[Ti_4O(OEt)_{14}(HOEt)]$

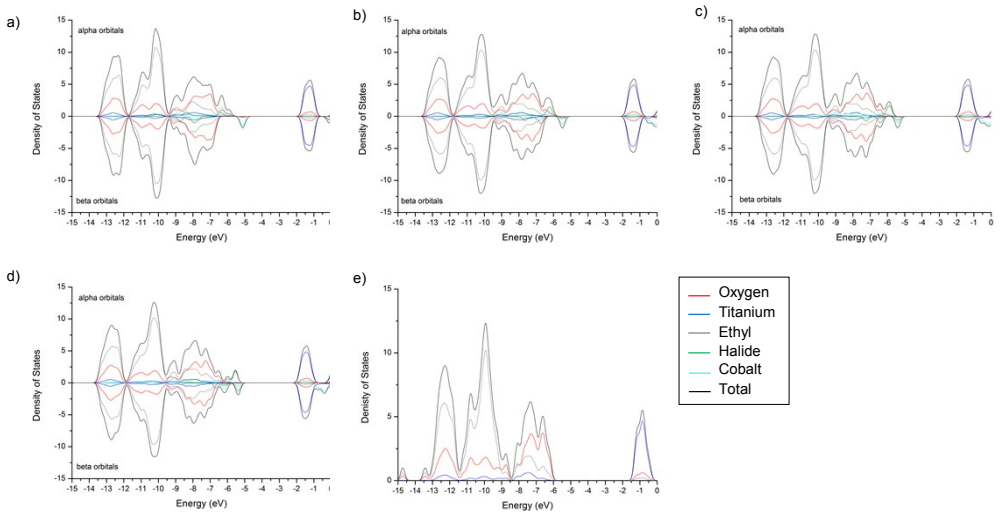

Figure S2: Density of states diagrams of $[Ti_4O(OEt)_{15}CoX]$ X = F (a), Cl (b), Br (c), I (d) and the undoped Ti_4 cage. Calculated on a B3LYP/6-31g*, 6-311g* (for iodine) level of theory. Spin-up (α orbitals) and spin-down channels (β orbitals) are distinguished by the positive and negative signs of DOS.

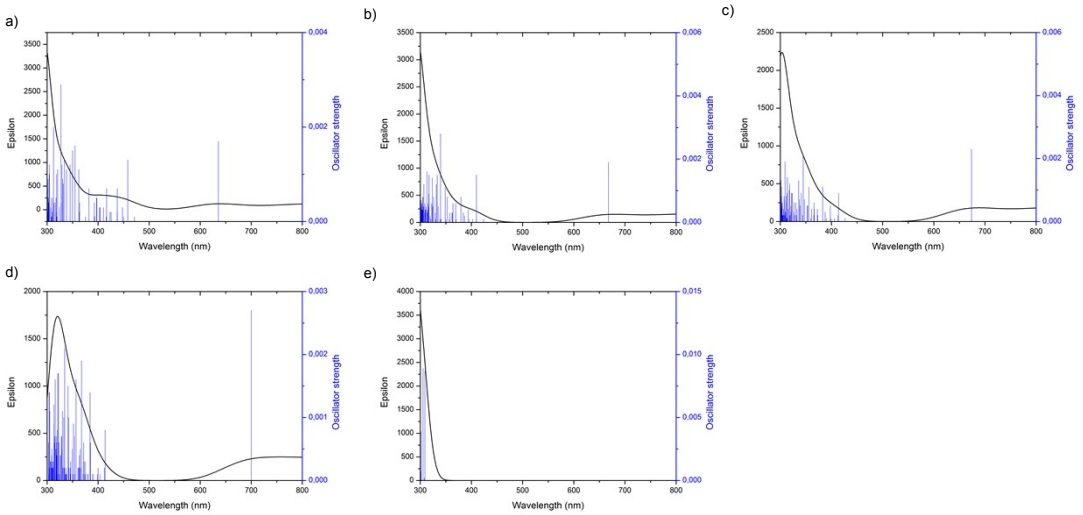

Figure S3: Calculated UV-Vis spectra of $[Ti_4O(OEt)_{15}CoX]$ X = F (a), Cl (b), Br (c), I (d) and the undoped $[Ti_4O(OEt)_{14}(HOEt)]$ cage (e) using TD-DFT methods (B3LYP/6-31g*, 6-311g* for iodine).

Table S11: Atomic composition of molecular orbitals of $[Ti_4O(OEt)_{15}CoF]$ (B3LYP/6-31g* level of theory).

Orbital	Orbital energy (eV)	Atomic composition (%)				
		Titanium	Cobalt	Oxygen	Fluorine	Ethyl
HOMO-α	-5.88	3	46	33	11	7
HOMO-α-1	-6.22	2	40	46	2	12
HOMO-α-4	-6.44	0	53	13	29	5
LUMO-α	-1.59	84	0	11	0	5
LUMO-α+1	-1.52	85	0	12	0	3
LUMO-α+2	-1.48	87	0	10	0	3
LUMO-α+3	-1.45	85	0	11	0	4
LUMO-α+4	-1.34	84	0	12	0	4
HOMO-β	-5.05	1	80	9	8	2
HOMO-β-1	-5.16	1	82	9	7	2
LUMO-β	-1.59	84	1	11	0	5
LUMO-β+1	-1.53	84	0	12	0	4
LUMO-β+14	0.32	69	13	10	0	8
LUMO-β+15	0.42	32	56	6	2	4
LUMO-β+16	0.67	56	24	10	1	9
LUMO-β+18	0.84	43	39	11	3	5

Table S12: Atomic composition of molecular orbitals of $[Ti_4O(OEt)_{15}CoCl]$ (B3LYP/6-31g* level of theory).

Orbital	Orbital energy (eV)	Atomic composition (%)				
		Titanium	Cobalt	Oxygen	Chlorine	Ethyl
HOMO-α	-6.08	1	31	24	35	6
HOMO-α-1	-6.19	0	19	4	74	3
HOMO-α-3	-6.44	1	27	53	6	12
LUMO-α	-1.70	85	0	10	0	5
LUMO-α+1	-1.59	84	0	11	0	4
LUMO-α+4	-1.46	84	0	12	0	4
HOMO-β	-5.42	1	69	9	19	2
HOMO-β-1	-5.42	1	70	10	17	2
LUMO-β	-1.71	85	1	9	0	5
LUMO-β+12	-0.48	31	62	4	2	1
LUMO-β+13	-0.17	6	85	5	1	3
LUMO-β+14	0.01	18	72	6	1	3
LUMO-β+16	0.40	53	27	11	2	7

Table S13: Atomic composition of molecular orbitals of $[Ti_4O(OEt)_{15}CoBr]$ (B3LYP/6-31g* level of theory).

Orbital	Orbital energy (eV)	Atomic composition (%)				
		Titanium	Cobalt	Oxygen	Bromine	Ethyl
HOMO-α	-5.84	0	13	2	82	3
HOMO-α-1	-5.86	0	17	6	75	3
LUMO-α	-1.69	85	0	10	0	5
LUMO-α+1	-1.59	85	0	11	0	4
LUMO-α+2	-1.53	86	0	11	0	3
LUMO-α+4	-1.46	84	0	12	0	4
HOMO-β	-5.34	0	55	7	35	2
HOMO-β-1	-5.45	1	58	9	31	2
HOMO-β-3	-6.48	0	32	10	53	5
LUMO-β	-1.71	84	1	10	0	5
LUMO-β+2	-1.54	84	2	10	0	3
LUMO-β+4	-1.50	81	3	12	0	3
LUMO-β+6	-1.34	84	2	11	0	3
LUMO-β+7	-1.28	83	1	12	0	4
LUMO-β+8	-1.23	83	1	13	0	4
LUMO-β+10	-1.10	82	0	13	0	4
LUMO-β+12	-0.54	28	66	4	2	1
LUMO-β+13	-0.24	6	84	6	2	3
LUMO-β+16	0.38	57	23	11	2	7

Table S14: Atomic composition of molecular orbitals of $[Ti_4O(OEt)_{15}CoI]$ (B3LYP/6-31g*, 6-311g* (for iodine) level of theory).

Orbital	Orbital energy (eV)	Atomic composition (%)				
		Titanium	Cobalt	Oxygen	Iodine	Ethyl
HOMO-α	-5.51	0	4	1	93	2
LUMO-α	-1.77	85	0	10	0	5
HOMO-β	-5.32	0	26	4	68	2
HOMO-β-1	-5.42	1	26	4	68	2
HOMO-β-2	-6.06	0	49	17	28	6
HOMO-β-3	-6.25	0	61	9	26	5
LUMO-β	-1.79	84	2	9	0	5
LUMO-β+4	-1.58	81	4	12	0	4
LUMO-β+5	-1.46	82	3	11	0	4
LUMO-β+8	-1.32	83	0	14	0	3
LUMO-β+13	-0.45	7	84	6	1	3
LUMO-β+14	-0.28	10	80	6	2	2

Table S15: Atomic composition of molecular orbitals of $[Ti_4O(OEt)_{14}(HOEt)]$ (B3LYP/6-31g* level of theory).

Orbital	Orbital energy (eV)	Atomic composition		
		Titanium	Oxygen	Ethyl
HOMO	-6.22	2	78	20
HOMO-1	-6.23	2	77	21
LUMO	-1.23	84	12	4
LUMO+1	-1.19	84	12	5
LUMO+2	-1.10	85	12	4

Table S16: Main orbital contributions to transition of $[Ti_4O(OEt)_{15}CoF]$ (with oscillator strengths ≥ 0.001). Calculated employing TD-DFT methods (B3LYP/6-31g*).

Main orbital contributions	Eg (eV)	Eg (nm)	Oscillator strength
HOMO-β-1 → LUMO-β+12 HOMO-β-1 → LUMO-β+15 HOMO-β-1 → LUMO-β+16 HOMO-β-1 → LUMO-β+18	1.956	635.6	0.0017
HOMO-β → LUMO-β HOMO-β → LUMO-β+1	2.707	458.0	0.0013
HOMO-α → LUMO-α HOMO-α → LUMO-α+1	3.496	354.7	0.0016
HOMO-α → LUMO-α+2 HOMO-α → LUMO-α+3	3.544	349.8	0.0015
HOMO-α-1 → LUMO-α+1 HOMO-α → LUMO-α+2 HOMO-α → LUMO-α+4	3.714	333.8	0.0013

Table S17: Main orbital contributions to transition of $[Ti_4O(OEt)_{15}CoCl]$ (with oscillator strengths ≥ 0.001). Calculated employing TD-DFT methods (B3LYP/6-31g*).

Main orbital contributions	Eg (eV)	Eg (nm)	Oscillator strength
HOMO-β-1 → LUMO-β+12 HOMO-β → LUMO-β+13	1.442	859.7	0.0013
HOMO-β-1 → LUMO-β+14 HOMO-β-1 → LUMO-β+16	1.857	667.8	0.0019
HOMO-α → LUMO-α+1	3.652	339.5	0.0028
HOMO-α-3 → LUMO-α+1 HOMO-α-3→ LUMO-α+4 HOMO-α-1 → LUMO-α	3.834	323.3	0.0014

Table S18: Main orbital contributions to transition of $[Ti_4O(OEt)_{15}CoBr]$ (with oscillator strengths ≥ 0.001). Calculated employing TD-DFT methods (B3LYP/6-31g*).

Main orbital contributions	Eg (eV)	Eg (nm)	Oscillator strength
HOMO-β-3 → LUMO-β+13 HOMO-β-1 → LUMO-β+12 HOMO-β → LUMO-β+13	1.427	868.91	0.0017
HOMO-β-1 → LUMO-β+14 HOMO-β-1 → LUMO-β+16	1.525	673.8	0.0023
HOMO-β → LUMO-β+2 HOMO-β → LUMO-β+4	3.239	382.8	0.0011
HOMO-β-1 → LUMO-β+6 HOMO-β-1 → LUMO-β+7 HOMO-β-1 → LUMO-β+8 HOMO-β-1 → LUMO-β+10	3.482	356.1	0.0011
HOMO-α-1 → LUMO-α+1	3.597	344.7	0.0021
HOMO-α-1 → LUMO-α+2 HOMO-α-1 → LUMO-α+4 HOMO-α → LUMO-α+1	3.691	335.9	0.0013

Table S19: Main orbital contributions to transition of $[Ti_4O(OEt)_{15}CoI]$ (with oscillator strengths ≥ 0.001). Calculated employing TD-DFT methods (B3LYP/6-31g*).

Main orbital contributions	Eg (eV)	Eg (nm)	Oscillator strength
HOMO-β-3 → LUMO-β+13 HOMO-β → LUMO-β+13	1.433	865.4	0.0021
HOMO-β-2 → LUMO-β+14 HOMO-β-1 → LUMO-β+14	1.771	700.0	0.0027
HOMO-α → LUMO-α HOMO-β → LUMO-β+4	3.227	384.2	0.0014
HOMO-β-1 → LUMO-β+5	3.374	367.4	0.0019
HOMO-β-1 → LUMO-β+8	3.475	356.8	0.0016

Table S20: Main orbital contributions to transition of $[Ti_4O(OEt)_{14}(HOEt)]$ (with oscillator strengths ≥ 0.001). Calculated employing TD-DFT methods (B3LYP/6-31g*).

Main orbital contributions	Eg (eV)	Eg (nm)	Oscillator strength
HOMO-1 → LUMO HOMO-1 → LUMO+1	4.013	308.9	0.0087
HOMO-1 → LUMO+1 HOMO → LUMO+1	4.060	305.4	0.0089
HOMO → LUMO	4.105	302.0	0.0039
HOMO-1 → LUMO+2	4.155	298.4	0.0059

3) $[Ti_7O_5(OEt)_{19}CoX]$ (X = F, Cl, Br, I) and $[Ti_7O_4(OEt)_{20}]$

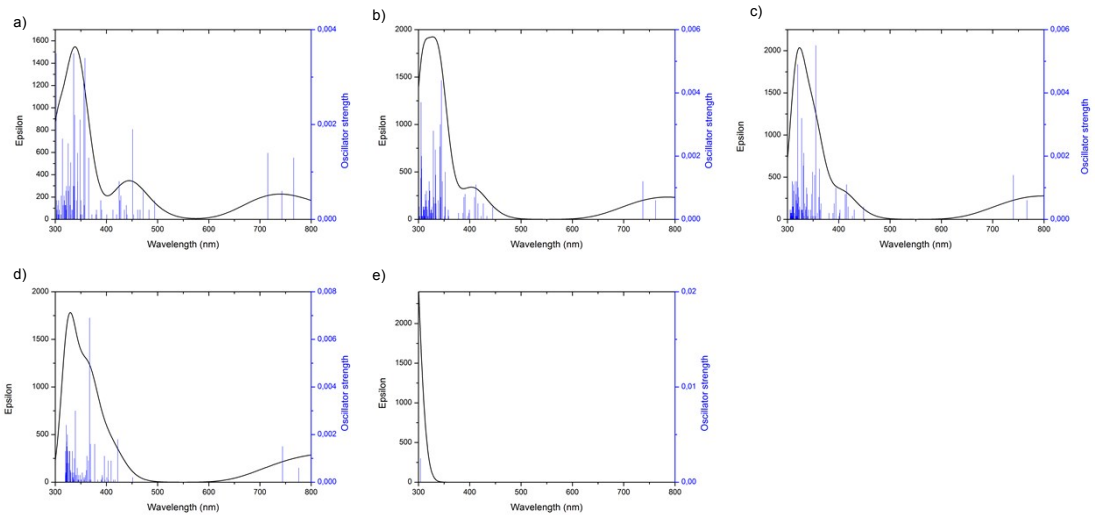

Figure S4: Calculated UV-Vis spectra of $[Ti_7O_5(OEt)_{19}CoX]$ X = F (a), Cl (b), Br (c), I (d) and $[Ti_7O_4(OEt)_{20}]$ (e) using TD-DFT methods (B3LYP/6-31g*, 6-311g* for iodine).

Table S21: Atomic composition of molecular orbitals of $[Ti_7O_5(OEt)_{19}CoF]$ (B3LYP/6-31g* level of theory).

Orbital	Orbital energy (eV)	Atomic composition (%)				
		Titanium	Cobalt	Oxygen	Fluorine	Ethyl
HOMO-α	-6.00	3	50	20	24	3
HOMO-α-1	-6.12	3	38	41	7	10
HOMO-α-2	-6.22	3	42	44	2	10
HOMO-α-4	-6.48	1	50	12	33	5
LUMO-α	-1.72	89	0	9	0	2
LUMO-α+1	-1.64	87	0	10	0	3
LUMO-α+2	-1.61	86	0	11	0	3
HOMO-β	-5.06	1	80	10	8	2
HOMO-β-1	-5.13	1	82	7	7	2
LUMO-β	-1.72	89	1	8	0	2
LUMO-β+1	-1.66	87	2	9	0	2
LUMO-β+2	-1.61	85	0	11	0	4
LUMO-β+4	-1.51	86	0	11	0	3
LUMO-β+14	-1.09	86	0	11	0	3
LUMO-β+15	-1.00	82	0	14	0	4
LUMO-β+16	-0.97	85	0	12	0	3
LUMO-β+17	-0.92	81	0	15	0	3
LUMO-β+18	-0.83	84	0	14	0	3
LUMO-β+22	0.005	62	27	7	1	3
LUMO-β+23	0.28	35	52	7	1	5
LUMO-β+25	0.39	50	33	10	2	6
LUMO-β+26	0.47	9	81	6	1	2

Table S22: Atomic composition of molecular orbitals of $[Ti_7O_5(OEt)_{19}CoCl]$ (B3LYP/6-31g* level of theory).

Orbital	Orbital energy (eV)	Atomic composition (%)				
		Titanium	Cobalt	Oxygen	Chlorine	Ethyl
HOMO-α	-6.13	1	29	14	52	3
HOMO-α-1	-6.16	0	22	7	68	3
HOMO-α-2	-6.17	0	22	12	62	3
HOMO-α-3	-6.41	3	28	46	12	11
HOMO-α-4	-6.44	3	30	50	5	12
LUMO-α	-1.80	90	0	9	0	2
LUMO-α+1	-1.72	87	0	9	0	2
HOMO-β	-5.40	1	67	10	20	2
HOMO-β-1	-5.48	1	71	7	19	2
LUMO-β	-1.80	89	1	8	0	2
LUMO-β+1	-1.76	86	3	9	0	2
LUMO-β+2	-1.70	58	0	11	0	4
LUMO-β+8	-1.40	83	0	13	0	2
LUMO-β+13	-1.19	85	0	13	0	2
LUMO-β+20	-0.30	25	58	5	2	2
LUMO-β+21	-0.20	14	76	6	1	2
LUMO-β+23	-0.01	45	40	13	1	2
LUMO-β+24	0.03	34	52	11	1	2

Table S23: Atomic composition of molecular orbitals of $[Ti_7O_5(OEt)_{19}CoBr]$ (B3LYP/6-31g* level of theory).

Orbital	Orbital energy (eV)	Atomic composition (%)				
		Titanium	Cobalt	Oxygen	Bromine	Ethyl
HOMO-α	-5.8	0	13	2	83	3
HOMO-α-1	-5.84	0	13	2	83	2
HOMO-α-2	-5.97	1	33	14	50	2
HOMO-α-4	-6.44	3	28	55	1	14
LUMO	-1.79	86	0	9	0	2
LUMO-α+1	-1.71	87	0	10	0	3
LUMO-α+2	-1.60	89	0	11	0	4
HOMO-β	-5.31	0	54	8	35	2
HOMO-β-1	-5.41	1	57	6	34	2
LUMO-β	-1.79	89	1	8	0	2
LUMO-β+1	-1.75	86	3	9	0	2
LUMO-β+7	-1.44	85	1	11	0	2
LUMO-β+13	-1.18	85	0	13	0	2
LUMO-β+20	-0.37	28	65	4	2	1
LUMO-β+21	-0.26	9	82	5	2	2
LUMO-β+23	-0.06	26	63	7	2	3

Table S24: Atomic composition of molecular orbitals of $[Ti_7O_5(OEt)_{19}CoI]$ (B3LYP/6-31g*, 6-311g* (for iodine) level of theory).

Orbital	Orbital energy (eV)	Atomic composition (%)				
		Titanium	Cobalt	Oxygen	Iodine	Ethyl
HOMO-α	-5.44	0	3	1	93	3
HOMO-α-1	-5.48	0	4	1	94	2
HOMO-α-2	-5.84	1	21	9	66	1
LUMO	-1.89	90	0	9	0	2
LUMO-α+1	-1.79	87	0	10	0	3
LUMO-α+5	-1.59	85	0	11	0	3
LUMO-α+6	-1.54	86	0	11	0	3
HOMO-β	-5.27	0	23	4	70	2
HOMO-β-1	-5.36	1	22	2	73	2
HOMO-β-2	-6.08	0	58	14	24	5
HOMO-β-3	-6.19	0	65	9	24	3
LUMO-β	-1.89	89	1	8	0	1
LUMO-β+1	-1.84	86	4	8	0	2
LUMO-β+21	-0.50	5	87	5	1	2
LUMO-β+22	-0.32	9	80	7	2	2

Table S25: Atomic composition of molecular orbitals of $[Ti_7O_4(OEt)_{20}]$ (B3LYP/6-31g* level of theory).

Orbital	Orbital energy (eV)	Atomic composition		
		Titanium	Oxygen	Ethyl
HOMO	-6.54	2	76	22
LUMO	-1.44	88	10	2
LUMO+1	-1.40	89	8	3

Table S26: Main orbital contributions to transition of $[Ti_7O_5(OEt)_{19}CoF]$ (with oscillator strengths ≥ 0.001). Calculated employing TD-DFT methods (B3LYP/6-31g*).

Main orbital contributions	Eg (eV)	Eg (nm)	Oscillator strength
HOMO-β-1 → LUMO-β+22 HOMO-β-1 → LUMO-β+26 HOMO-β → LUMO-β+23 HOMO-β → LUMO-β+25	1.619	765.9	0.0013
HOMO-β-1 → LUMO-β+1 HOMO-β-1 → LUMO-β+26	1.733	715.2	0.0014
HOMO-β-1 → LUMO-β+1 HOMO-β-1 → LUMO-β+2 HOMO-β → LUMO-β+4	2.748	451.1	0.0019
HOMO-α → LUMO-α	3.394	365.3	0.0013
HOMO-α-1 → LUMO-α HOMO-α → LUMO-α+1	3.462	358.1	0.0034
HOMO-α-4 → LUMO-α HOMO-α → LUMO-α+1	3.486	355.7	0.0029
HOMO-α-2 → LUMO-α HOMO-α → LUMO-α+2	3.557	348.6	0.0021
HOMO-α-1 → LUMO-α+1 HOMO-β-1 → LUMO-β+14 HOMO-β-1 → LUMO-β+17	3.610	343.4	0.0014
HOMO-α-2 → LUMO-α+1	3.669	337.9	0.0022

HOMO-α-2 → LUMO-α+2 HOMO-β-1 → LUMO-β+15			
HOMO-α-1 → LUMO-α+2 HOMO-β → LUMO-β+16 HOMO-β → LUMO-β+18	3.691	335.9	0.0035

Table S27: Main orbital contributions to transition of $[Ti_7O_5(OEt)_{19}CoCl]$ (with oscillator strengths ≥ 0.001). Calculated employing TD-DFT methods (B3LYP/6-31g*).

Main orbital contributions	Eg (eV)	Eg (nm)	Oscillator strength
HOMO-β-1 → LUMO-β+20 HOMO-β → LUMO-β+21	1.504	824.5	0.0019
HOMO-β-1 → LUMO-β+20 HOMO-β-1 → LUMO-β+23 HOMO-β-1 → LUMO-β+24	1.682	737.3	0.0012
HOMO-β-1 → LUMO-β+1 HOMO-β-1 → LUMO-β+2	3.010	411.9	0.0011
HOMO-α-2 → LUMO-α HOMO-α-1 → LUMO-α HOMO-α → LUMO-α	3.520	352.2	0.0015
HOMO-α-3 → LUMO-α HOMO-α-2 → LUMO-α HOMO-α → LUMO-α	3.577	346.6	0.0012
HOMO-α-4 → LUMO-α HOMO-α → LUMO-α+1	3.596	344.8	0.0044
HOMO-β-1 → LUMO-β+8 HOMO-β-1 → LUMO-β+13	3.628	341.7	0.0023
HOMO-α-3 → LUMO-α+1 HOMO-α-2 → LUMO-α+1 HOMO-α-1 → LUMO-α+1	3.716	333.7	0.0014

Table S28: Main orbital contributions to transition of $[Ti_7O_5(OEt)_{19}CoBr]$ (with oscillator strengths ≥ 0.001). Calculated employing TD-DFT methods (B3LYP/6-31g*).

Main orbital contributions	Eg (eV)	Eg (nm)	Oscillator strength
HOMO-β → LUMO-β+21	1.480	837.7	0.0025
HOMO-β-1 → LUMO-β+20 HOMO-β-1 → LUMO-β+23	1.675	740.1	0.0014
HOMO-β → LUMO-β+7	3.144	394.4	0.0010
HOMO-α-2 → LUMO-α HOMO-α → LUMO-α	3.421	362.4	0.0016
HOMO-α-2 → LUMO-α+1 HOMO-α-2 → LUMO-α+2 HOMO-α → LUMO-α+1	3.49	355.5	0.0055
HOMO-α-2 → LUMO-α+1 HOMO-α → LUMO-α+1	3.513	353.9	0.0014
HOMO-α-1 → LUMO-α+1	3.554	348.8	0.0015
HOMO-α-4 → LUMO-α	3.677	337.2	0.0010
HOMO-α-4 → LUMO-α HOMO-α → LUMO-α+5 HOMO-α→ LUMO-α+6	3.737	331.8	0.0021

Table S29: Main orbital contributions to transition of $[Ti_7O_5(OEt)_{19}CoI]$ (with oscillator strengths ≥ 0.001). Calculated employing TD-DFT methods (B3LYP/6-31g*, 6-311g* for iodine).

Main orbital contributions	Eg (eV)	Eg (nm)	Oscillator strength
HOMO-β-3 → LUMO-β+21 HOMO-β-2 → LUMO-β+21 HOMO-β → LUMO-β+21	1.422	871.8	0.0031
HOMO-β-3 → LUMO-β+22 HOMO-β-2 → LUMO-β+22 H OMO-β-1 → LUMO-β+22	1.668	743.4	0.0015
HOMO-β-1 → LUMO-β+1	2.941	421.6	0.0018
HOMO-β → LUMO-β+7	3.132	395.8	0.0011
HOMO-α-2 → LUMO-α	3.274	376.8	0.0016
HOMO-α → LUMO-α+5 HOMO-α → LUMO-α+6	3.363	368.6	0.0016
HOMO-α-2 → LUMO-α+1	3.380	366.8	0.0069
HOMO-β-2 → LUMO-β	3.429	361.6	0.0011

Table S30: Main orbital contributions to transition of $[Ti_7O_4(OEt)_{20}]$ (with oscillator strengths ≥ 0.001). Calculated employing TD-DFT methods (B3LYP/6-31g*).

Main orbital contributions	Eg (eV)	Eg (nm)	Oscillator strength
HOMO → LUMO HOMO → LUMO+1	4.081	303.8	0.0025
HOMO → LUMO+1	4.174	297.1	0.0154

4) Diffuse reflectance UV-vis spectroscopy

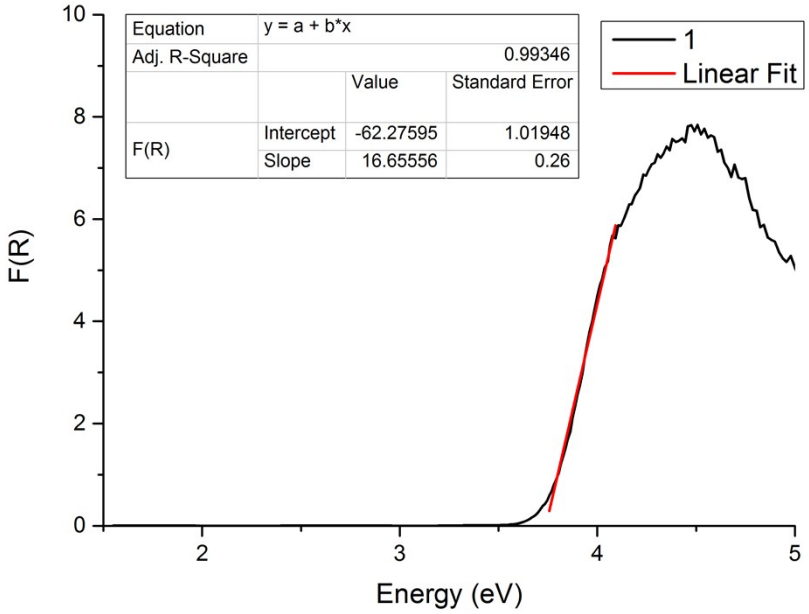

Figure S5: Diffuse reflectance UV-vis spectrum of $[Ti_3O(O^iPr)_9(OMe)]$ and linear fit to determine band gap.

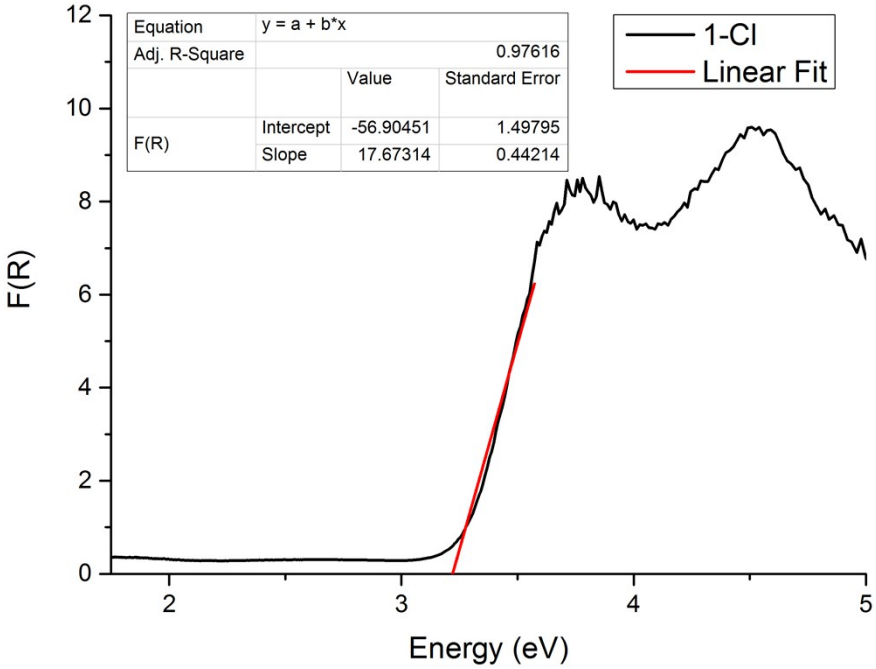

Figure S6: Diffuse reflectance UV-vis spectrum of $[Ti_3O(O^iPr)_9Cl]$ and linear fit to determine band gap.

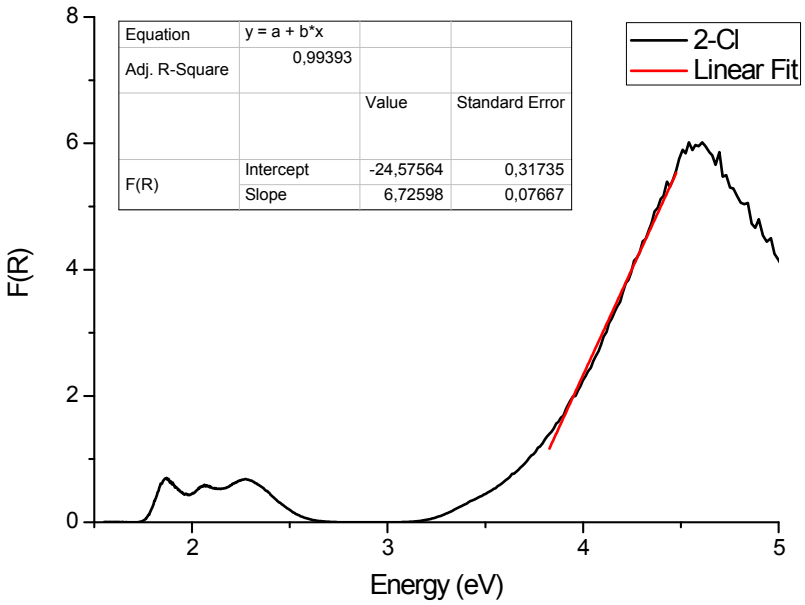

Figure S7: Diffuse reflectance UV-vis spectrum of $[Ti_4O(OEt)_{15}CoCl]$ and linear fit to determine band gap.

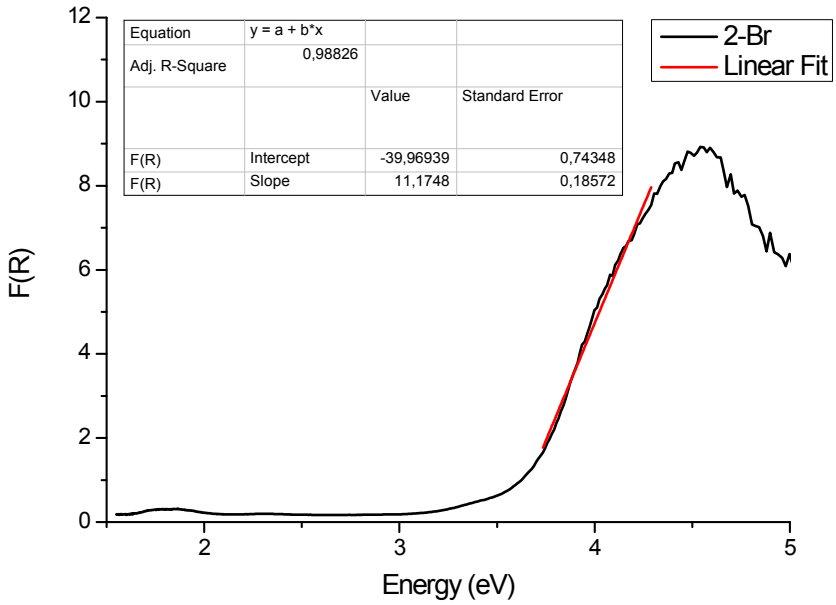

Figure S8: Diffuse reflectance UV-vis spectrum of $[Ti_4O(OEt)_{15}CoBr]$ and linear fit to determine band gap.

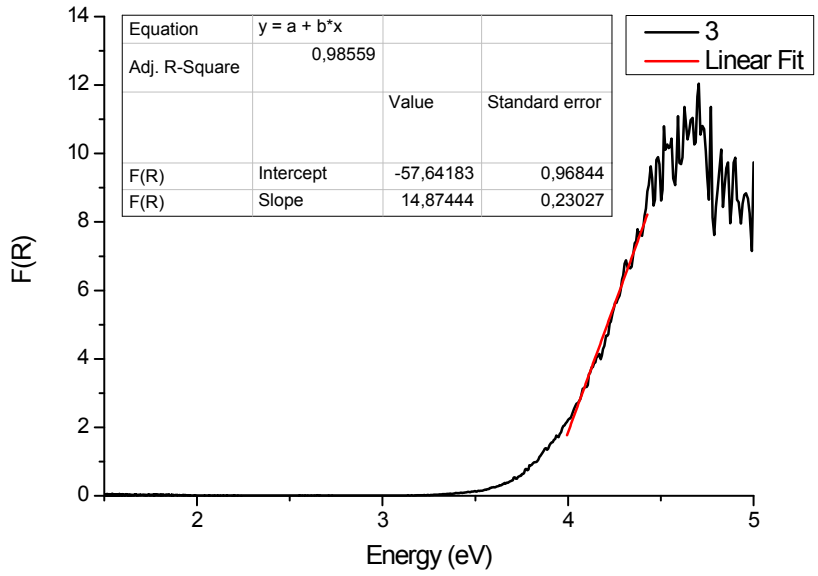

Figure S9: Diffuse reflectance UV-vis spectrum of $[Ti_7O_4(OEt)_{20}]$ and linear fit to determine band gap.

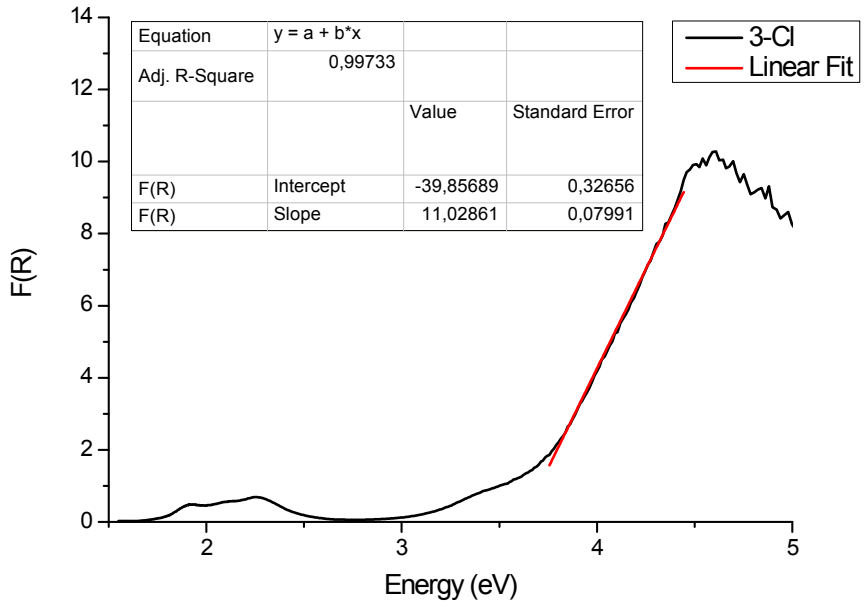

Figure S10: Diffuse reflectance UV-vis spectrum of $[Ti_7O_5(OEt)_{19}CoCl]$ and linear fit to determine band gap.

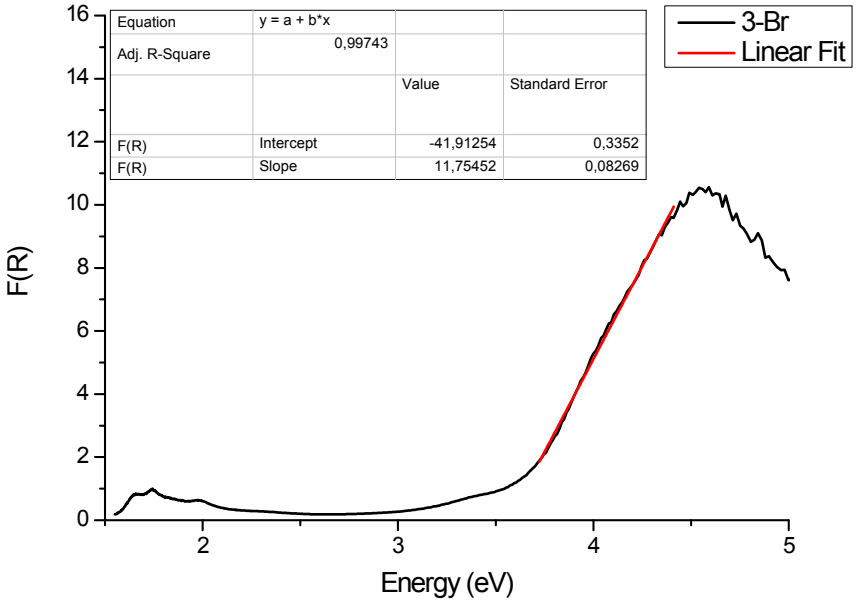

Figure S11: Diffuse reflectance UV-vis spectrum of $[Ti_7O_5(OEt)_{19}CoBr]$ and linear fit to determine band gap.

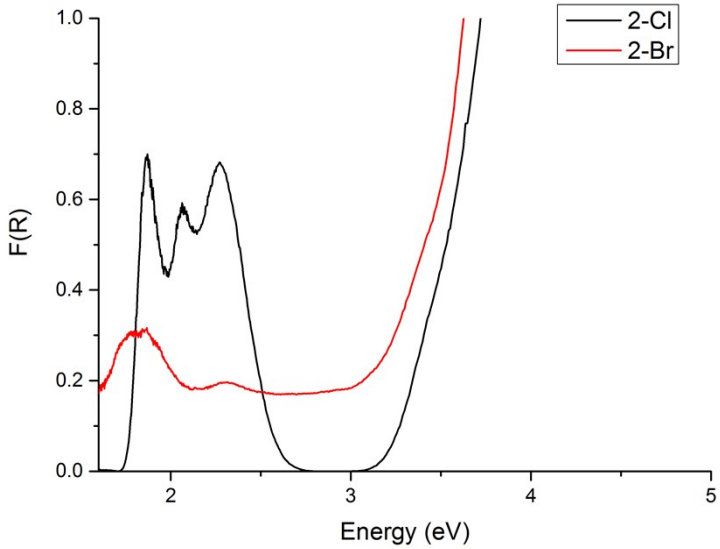

Figure S12. An expanded 500-700 nm region of diffuse reflection spectra for **2**-Cl and **2**-Br showing the absorbances for **2**-Br.

5) Single-crystal X-ray crystallography

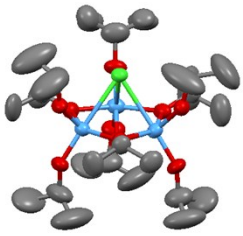

Figure S13: Structure of **1**-Cl. Displacement ellipsoids are drawn at the 50% probability level. H omitted for clarity. Blue = Ti, green = Cl, red = O, grey = C.

Table S31: Crystallographic data for **1**-Cl.

Compound	**1**-Cl
Empirical formula	$C_{27}H_{63}ClO_{10}Ti_3$
Formula weight	726.92
Temperature	180(2) K
Wavelength	0.7107 Å
Crystal system	Tetragonal
Space group	$P4_12_12$
Unit cell dimensions	a = 12.54740(10) Å
	b = 12.54740(10) Å
	c = 49.8245(5) Å
	α = 90°
	β = 90°
	γ = 90°
Volume	7844.23(15) Å^3
Z	8
Absorption coefficient	0.707 mm^{-1}
Crystal size	0.370 x 0.160 x 0.150 mm^3
Reflections collected	20677
Independent reflections	6324 [$R_{(int)}$ = 0.0554]
Goodness-of-fit on F2	1.05
Final R indices [I>2σ(I)]	R_1 = 0.0598, wR_2 = 0.1507
R indices (all data)	R_1 = 0.0970, wR_2 = 0.1671